See related Commentary on page 1586

The American Journal of Pathology, Vol. 176, No. 4, April 2010

DOI: 10.2353/ajpath.2010.091071

Cardiovascular, Pulmonary and Renal Pathology

Adriamycin Nephropathy

A Failure of Endothelial Progenitor Cell-Induced Repair

Kaoru Yasuda,* Hyeong-Cheon Park,* Brian Ratliff,* Francesco Addabbo,*† Antonis K. Hatzopoulos,‡ Praveen Chander,§ and Michael S. Goligorsky*

From the Renal Research Institute, Division of Nephrology, Departments of Medicine and Pharmacology, and the Department of Pathology,§ New York Medical College, Valhalla, New York; the Department of Pharmacology,† University of Bari, Italy; and the Department of Medicine, Division of Cardiovascular Medicine and the Department of Cell & Developmental Biology,‡ Vanderbilt University, Nashville, Tennessee*

Adriamycin-associated nephropathy (AAN) remains poorly understood. We hypothesized that adriamycin affects endothelial progenitor cells (EPCs), leading to impaired regeneration. We analyzed renal hematopoietic stem cells (HSCs) and EPCs in mice with AAN and examined the potential contribution of adoptive transfer of intact EPCs to the repair processes. FACS analyses revealed that populations of HSCs and EPCs were scarcely represented in control kidneys and did not change numerically in kidneys obtained from mice with AAN. The observed defect in engraftment was attributable to the decreased viability and increased senescence of EPCs. Adoptive transfer of intact EPCs improved proteinuria and renal function, with a threefold decrease in mortality. Infusion of EPCs to adriamycin-treated mice reduced plasma levels of interleukin-1α and -β and granulocyte-colony stimulating factor as well as increased the level of vascular endothelial growth factor with concomitant improvement of vascular density and reduction of apoptosis. An additional mechanism of tissue repair is proposed based on tunneling nanotube formation between EPCs and endothelial cells exposed to adriamycin, leading to the multiple rounds of exchange between EPCs and mature cells. In conclusion, AAN is associated with development of EPC incompetence; adoptive transfer of intact EPCs blunts morphological and functional manifestations of AAN; and the proposed mechanisms of repair by EPCs include direct incorporation into blood vessels, paracrine signaling, and tunneling nanotube renewal of mitochondrial pool in endothelial cells. ***(Am J Pathol 2010, 176:1685–1695; DOI: 10.2353/ajpath.2010.091071)***

Molecular pharmacology profile of anthracycline antibiotic Adriamycin (Doxorubicin) includes inhibition of nucleic acid synthesis and cytochrome *c* oxidase, intercalation of DNA, and generation of reactive oxygen species, which account not only for its oncolytic effects but also for the depression of the bone marrow and development of cardiomyopathy and nephropathy.[1–3] While cardiotoxicity is a major limiting factor in the use of this chemotherapeutic agent, adriamycin-associated nephropathy (AAN) contributes significantly to its toxicologic profile. Toxicity of anthracyclines in general is poorly understood.[2] AAN has been variably attributed to complement activation, increased production of reactive oxygen species, reduction in heparan sulfate and increased heparanase expression in glomeruli, and dysregulation of renin-angiotensin system,[4,5] as well as activation of p38 MAP kinase and TGF-beta1/Smad signaling,[6] among other proposed mechanisms. It is instructive that the kidney-resident side population cells, capable of multilineage differentiation, as well as the main population cells (devoid of side-population cells) adoptively transferred to mice with AAN resulted in the reduction of proteinuria.[7] These studies raised a legitimate question whether adriamycin affects not only the bone marrow hematopoietic stem cells (HSCs), but also bone marrow–derived and

Supported in part by National Institutes of Health grants DK54602, DK052783, and DK45462 (to M.S.G.) and Westchester Artificial Kidney Foundation.

Accepted for publication December 10, 2009.

K.Y. and H.-C.P. contributed equally to this study.

Current address for H.-C.P.: Department of Internal Medicine, Yonsei University College of Medicine, Seoul, Korea; for F.A.: Department of Pharmacology, University of Bari, Italy.

Address reprint requests to Michael S. Goligorsky, M.D., Ph.D., Renal Research Institute, Division of Nephrology, Departments of Medicine and Pharmacology, New York Medical College, Valhalla, NY 10595. E-mail: Michael_goligorsky@nymc.edu.

renal-resident stem and/or endothelial progenitor cells and whether this injury may provide explanation for the progressive nature of AAN. Here, we analyzed quantitatively and qualitatively stem and endothelial progenitor cells, (consensually characterized as HSCs based on the co-expression of surface markers CD150 and CD117 [c-Kit] or endothelial progenitor cells [EPCs] based on the co-expression of surface markers CD34 and Flk-1 with or without CD45 expression) present in the kidneys of mice with AAN and examined the potential contribution of adoptive transfer of intact endothelial progenitor cells to the repair processes.

Materials and Methods

Animals and Induction of AAN

All animal protocols were conducted in accord with the National Institutes of Health guidelines and were approved by the Institutional Animal Care Committee. Male 8- to 12-week-old BALB/c mice (Jackson Labs, Bar Harbor, ME) were housed under 12-hour light:dark cycle, fed a regular chow, and received water *ad lib*. Animals received tail vein injection of 10.2 mg/kg adriamycin to induce AAN. An additional group of mice was treated with EPCs by adoptive transfer of approximately 5×10^5 cultured EPCs injected into the circulation via the tail vein on the day 5 postadriamycin. Nontreated mice received an injection of normal saline. On days 0, 4, and 10 and at 2 and 3 weeks, mice were placed in metabolic cages for 24-hour urine collection. Mice were sacrificed at 3 weeks after adriamycin injection. On the day of sacrifice, after Ketamin/Xylazine anesthesia, blood was obtained through left ventricular puncture and animals were perfused with normal saline followed by perfusion-fixation with 4% paraformaldehyde for morphological studies. Alternatively, fixation step was omitted and mice were used for stem cell isolation, as detailed below.

Cell Isolation from the Kidney and FACS Analysis

For stem cell isolation, single-cell suspension was prepared from the whole kidney. Kidneys from each experimental group were placed in 2 ml of ice-cold RPMI 1640 (Invitrogen, Carlsbad, CA) and minced using a sterile scalpel. Digestion of the tissue was performed in collagenase II (Invitrogen) solution (1 mg/ml of RPMI 1640) for 30 minutes at 37°C in 5% CO_2. Cell suspensions were passed through a 35-μm nylon sieve. Repeated digestions were performed until microscopic evaluation showed a suspension of single cells. Finally, cells were washed in PBS-BSA 1% (w/v), counted, and kept on ice in the dark.

FACS analysis was performed to quantify the dynamics of EPCs and HSCs in AAN model. For this analysis, 1×10^6 cells from the single-cell suspensions were incubated with specified primary antibodies for 1 hour at 4°C in the dark. The following antibodies were used for incubation: FITC-conjugated anti-mouse CD34, PE-conjugated anti-mouse Flk-1, PE-conjugated anti-mouse CD150, FITC-conjugated anti-mouse CD117 (c-Kit; BD Pharmingen, San Diego, CA). After each incubation step, cells were washed with PBS-BSA 1% (w/v) and finally fixed in 1% paraformaldehyde. Data were acquired using a FACScan cytometer equipped with a 488-nm argon laser and a 635-nm red diode laser and analyzed using CellQuest software (Becton Dickinson, Franklin Lakes, NJ). The set-up of FACScan was performed using unstained cells. For quantification of EPCs and HSCs, the number of CD34/Flk-1 and CD150/c-Kit double-positive cells within the monocytic cell population was counted.

Preparation of EPCs and Cell Culture

To isolate bone marrow mononuclear cells, cells were obtained by flushing the tibias and femurs of BALB/c mice with PBS and density gradient centrifugation with Histopaque-1077 (Sigma Chemical Co., St. Louis, MO) was performed. Bone marrow mononuclear cells were cultured in Mouse Endothelial Progenitor Cell Culture Serum-Free Media (Celprogen, San Pedro, CA) on dishes coated with 10 μg/ml pronectin (Sigma, St Louis, MO). After 3 days in culture, nonadherent cells were removed, and medium exchanged every 2 days. Thus prepared cells were further characterized to ensure the purity of EPC population (>95% of cells are labeled by these markers) by (1) uptake of DiI-labeled acetylated low-density lipoprotein (2.4 μg/ml of Dil-Actylated-LDL, Biomedical Technologies, Inc., Stoughton, MA), and (2) Lectin binding (25 μg/ml of Fluorescein-*Ulex Europeus* Lectin, Biomeda Corp., Forster City, CA). Colony-forming unit assay was performed according to the previously described protocol.[8] Briefly, 1×10^5 bone marrow mononuclear cells were plated on pronectin-coated dishes and 2 weeks later colonies (>50 cells) were counted. Cells were also stained for the expression of CD31. In some *in vitro* experiments, mouse embryonic EPCs, previously established and characterized,[9] were used.

To detect apoptotic and necrotic cells, FACS analysis using fluorescein isothiocyanate-Val-Ala-Asp (OMe)-fluoromethylketone (FITC-VAD-FMK, Calbiochem, La Jolla, CA) and 7-Aminoactinomycin D (7-AAD, Invitrogen) was performed. Detection of cell senescence was accomplished by staining for senescence-associated β galactosidase (SA-β-gal).

Morphological Analyses

Kidneys were collected from mice at 3 weeks after adriamycin injection for morphological analysis. Midcoronal kidney sections were fixed in 4% paraformaldehyde and embedded in paraffin. Paraffin sections (4 μm thick) were stained with hematoxylin and eosin, periodic acid-Schiff, and Masson trichrome and examined by a nephropathologist blinded to the origin of individual preparations. Semiquantitative grading of injury, designed to evaluate the degree of glomerular injury (segmental sclerosis, podocyte hypertrophy, and proliferation) and tubulointerstitial injury (tubular casts, debris, necrosis, and

interstitial fibrosis), was used. The degree of injury and fibrosis score ranging from 0 to 3 was determined as follows: 0, normal kidney; 1, mild changes; 2, moderate changes; 3, severe changes. The scores were determined in each section selected at random, and >20 fields were examined under ×100 magnification. Data are presented as a sum of individual pathological scores, each obtained in 5 different mice.

For immunohistochemical detection of renal vasculature, cryosections were stained with endothelial-specific antibodies – CD31 (BD Phermingen, San Diego, CA) and von Willebrand factor (Dako, Glostrup, Denmark). Terminal deoxynucleotidyl transferase-mediated dUTP nick-end labeling (TUNEL) staining kit (Calbiochem FragEL DNA Fragmentation Detection Kit, La Jolla, CA) was used to detect apoptotic cells in paraffin sections, according to manufacturer's instructions.

Multiplex Analysis of Cyto- and Chemokines

Profiling of cyto- and chemokines and vascular endothelial growth factor (VEGF) release was accomplished using multiplex analysis of the plasma obtained from experimental animals (Luminex Inc, Austin TX). The following parameters were determined: interleukin (IL)-1α, IL-1β, IL-2, IL-4, IL-5, IL-6, IL-7, IL-9, IL-10, IL-12(p70), IL-13, IL-15, IL-17, interferon-γ, interferon-γ–inducible protein (IP-10), granulocyte-colony stimulating factor (G-CSF), granulocyte-macrophage-colony stimulating factor, tumor necrosis factor-α, keratinocyte chemoattractant (KC), monocyte chemoattractant protein, macrophage inflammatory protein, and regulated on activation normal T cell expressed and secreted (RANTES) as previously detailed by us.[10] The plates were analyzed using Luminex IS100 analyzer. The data were saved and evaluated as median fluorescence intensity using appropriate curve-fitting software (Luminex 100IS software version 2.3). A 5-parameter logistic method with weighting will be used, as a part of the software routine.

For measurement of plasma VEGF, we used ELISA Development kit (Peprotech, Rocky Hill, NJ) with 96-well ELISA microplates (Nunc MaxiSorp, Rochester, NY) and 2,2′-azinobis-(3-ethyl-benzothiazoline-6-sulfonic acid; Sigma, St Louis, MO).

Analytical Protocols

Urine albumin content was determined with a Bio-Rad Protein Assay with BSA standards (Bio-Rad, Hercules, CA), and urine and serum creatinine were determined with a Creatinine Assay kit (Cayman Chemical, Ann Arbor, MI). Proteinuria was expressed as urine protein/creatinine ratio.

EPC Labeling and Tracing in AAN Model

To track injected EPCs in the tissues after engraftment, cells were labeled with carboxyfluorescein diacetete succinimidyl ester (CFDA SE, Invitrogen, Carlsbad, CA). For this purpose, EPCs were washed once with PBS and resuspended in 10 μmol/L CFDA SE/PBS for 15 minutes at 37°C. After labeling, the cells were washed twice in PBS, and injected via the tail vein. To examine their incorporation, the kidneys were removed on day 21, and costained with CD31 monoclonal antibody (BD Phermingen), followed by Alexa fluor–labeled antibodies against rat IgG (Invitrogen, Carlsbad, CA).

Statistical Analysis

Statistical analysis was performed using software program, GraphPad Prism 4 (Software Inc, San Diego, CA). For survival analysis, percent survival was analyzed using Kaplan–Meier method. The statistical significance of the survival experiments was determined using the log-rank test. Non-normally distributed data were analyzed by nonparametric Mann–Whitney *U* test. Multiple group comparisons were performed using one-way or two-way analysis of variance with *post hoc* Bonferroni correction. Values of $P < 0.05$ were considered statistically significant. All values are expressed as mean ± SEM.

Results

The Fate of Renal Stem/Progenitor Cells in AAN

Mice developed progressive elevation of serum creatinine and worsening proteinuria after adriamycin injection and exhibited an increased mortality rate, as illustrated by Kaplan–Meier survival curve (Figure 1, A–C).

Morphological analysis of kidneys obtained from adriamycin-injected mice revealed focal podocyte proliferation with epithelial-to-fibroepithelial adhesions to the Bowman capsule, frequent podocytic hypertrophy with occasional vacuolization, and rare segmental sclerosis. Glomeruli appeared slightly swollen with mild-to-moderate (1 to 2+) endocapillary and podocytic hypertrophy and with Bowman spaces focally containing proteinaceous material. Tubules were frequently dilated, contained variable numbers of hyaline casts, and showed widespread degeneration and focal epithelial necrosis (Figure 2, A and B).

The population of CD34+Flk-1+ cells (approximately 50% of these cells did not express CD45 and presumed to be EPCs) harvested from the kidney equaled 0.04% of the total cellular endowment in control mice and showed a modest elevation on day 14 postinjection of adriamycin (0.087%; Figure 3A). However, at day 21 of AAN the population of EPCs in the kidney was indistinguishable from the baseline (Figure 3B). FACS analyses of different subsets of stem and progenitor cells revealed that the population of HSCs (c-Kit+/CD150+) was represented in control kidneys by 0.043% of total cell number. This population did not change numerically in kidneys obtained from mice with AAN (Figure 3C), averaging on day 14 postinjection 0.073% and on day 21 0.02%.

The observed lack of an expected surge of stem/progenitor cells engrafting the AAN kidneys could not be attributed to the loss of the stromal cell–derived factor-1 (SDF-1) production, because immunohistochemical staining of the kidneys showed its enhanced expression

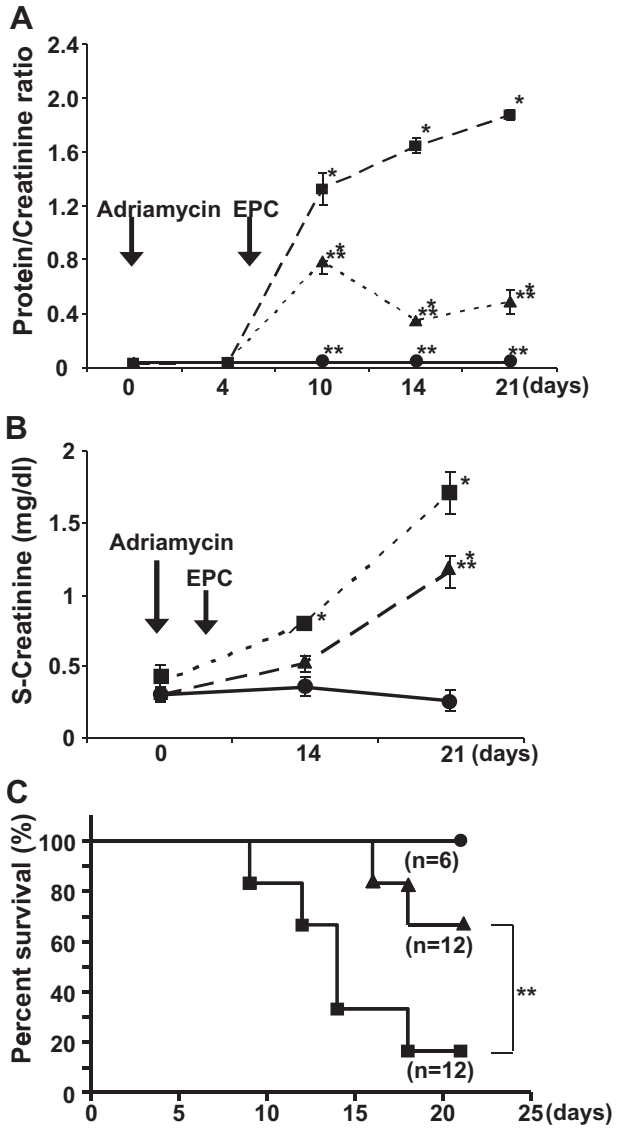

Figure 1. Renal function and survival of mice treated with adriamycin. **Circles** indicate control; **squares**, adriamycin; **triangles**, adriamycin followed by adoptive transfer of EPCs. **Arrows** indicate the time of infusion of adriamycin and EPCs. **A:** Urine protein:creatinine ratio. **B:** Serum creatinine concentration. * and ** denote $P < 0.05$ versus control and versus adriamycin, respectively ($n = 18$ each group). **C:** Kaplan–Meier survival curve. **$P < 0.05$ versus adriamycin, Logrank test: $P < 0.05$.

in the cortical and medullary areas (Figure 4A). In contrast to this, the clonogenicity of EPCs was perturbed: colony-forming unit assay using EPCs obtained from mice receiving adriamycin showed a significant suppression of this function compared with control (Figure 4B), suggesting that the adriamycin-induced functional incompetence of EPCs may participate in the defective engraftment and, consequently, impaired regenerative capacity.

To address the cause(s) of functional incompetence, we examined *in vitro* the viability of EPCs after adriamycin administration. The rate of apoptosis (detected by FACS analysis using FITC-VAD-FMK) in cultured EPCs treated with various doses of adriamycin was increased already at the concentration of 1 μmol/L, whereas necrosis (as judged by FACS analysis of 7-AAD staining) was detectable at 10 μmol/L adriamycin (Figure 5A). EPCs treated with adriamycin also showed signs of stress-induced premature senescence, as judged by the results of staining for senescence-associated β-galactosidase (Figure 5B). Collectively, these findings suggested that EPCs are targeted by this anthracyclin antibiotic to limit their viability or develop cell cycle arrest, thus explaining in part the results of colony forming unit assay.

Adoptive Transfer of EPCs to Mice with AAN

To gain further insights into the possibility of the failed EPC-induced regeneration in adriamycin nephropathy, in the next series of experiments mice received transfusion of EPCs obtained from healthy age- and gender-matched BALB/c donors. EPCs were isolated, maintained, and expanded as detailed in the Methods. Mice received injection of approximately 5×10^5 cells on day 5 after adriamycin injection, at the time when no significant proteinuria was yet detectable. This protocol resulted in a dramatic improvement in proteinuria and a moderate but significant improvement of renal function, as judged by the serum creatinine, 2 to 3 weeks postinitiation of AAN (Figure 1, A and B). Moreover, the overall mortality was decreased almost threefold by 3 weeks (Figure 1C).

Morphological studies of the kidneys obtained from mice that received adriamycin followed by EPC infusion revealed no focal segmental glomerulosclerotic lesions and marked attenuation of podocytic hypertrophy, vacuolization, and proliferation. Glomerular and cellular swelling was also attenuated (0.5 to 1.5+) compared with mice that did not receive EPCs. Rare finding of protein in the Bowman's space was present. Tubular damage was markedly reduced (Figure 2, A and B).

A single systemic injection of EPCs was accompanied by a dramatic increase in HSCs and EPCs in the affected kidneys (Figure 3, B and C). The population of HSCs, which was not changed in the kidneys of adriamycin-injected mice, was dramatically enriched (more than sevenfold) in mice receiving EPC transplantation. This latter group also showed elevation in HSCs in the spleen and bone marrow, reaching the level found in untreated animals (not shown). EPCs in the kidneys of adriamycin-treated mice receiving cell therapy showed a progressive increase, whereas increase was maximal on day 14 in the spleen and day 21 in the bone marrow, perhaps reflecting the trafficking of these cells from the bone marrow to the spleen and the kidney (not shown).

Sites of Engraftment of EPCs and Potential Mechanisms of Repair

The injected CFDA-tagged EPCs engrafting the kidney were detectable mostly in the cortical and medullary microvasculature (Figure 6A). In the cortex, EPCs were frequently observed in the glomeruli and peritubular capillaries and rarely in the tubules. In the medulla, EPCs were detectable in the vasae rectae, as judged by the

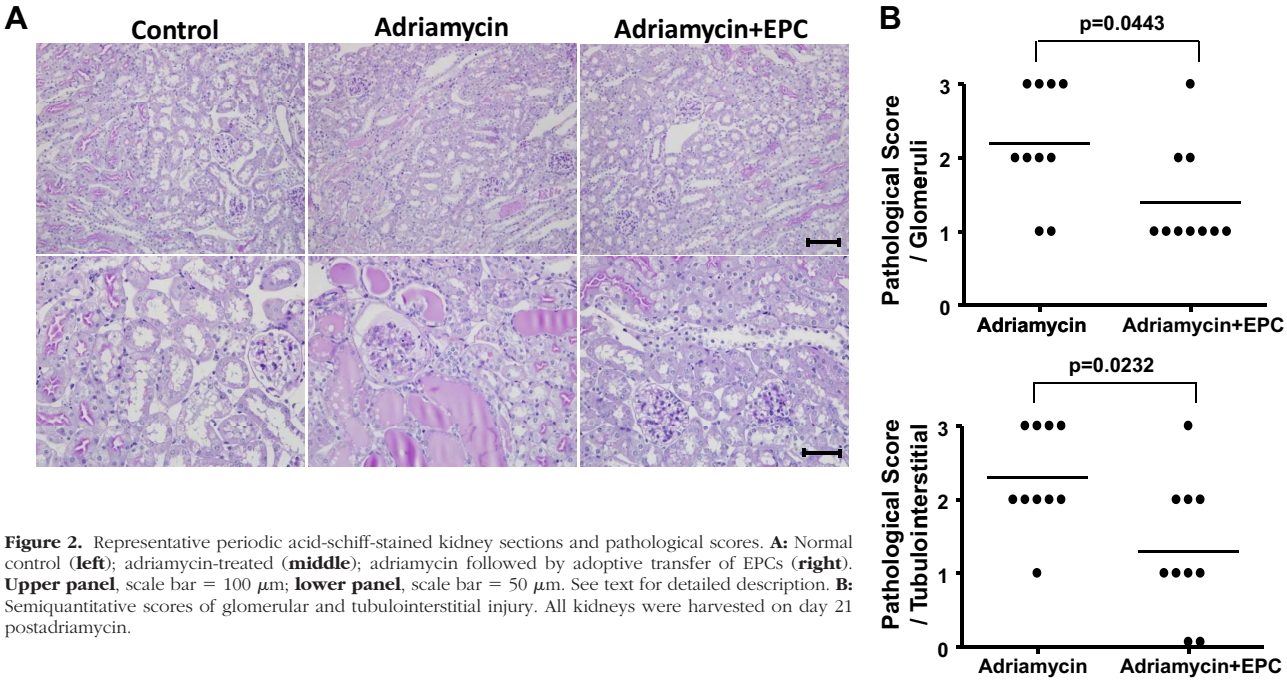

Figure 2. Representative periodic acid-schiff-stained kidney sections and pathological scores. **A:** Normal control (**left**); adriamycin-treated (**middle**); adriamycin followed by adoptive transfer of EPCs (**right**). **Upper panel**, scale bar = 100 μm; **lower panel**, scale bar = 50 μm. See text for detailed description. **B:** Semiquantitative scores of glomerular and tubulointerstitial injury. All kidneys were harvested on day 21 postadriamycin.

co-localization of transplanted cells with CD31-stained cells. The approximate number of EPCs engrafting the kidney in AAN was quantified by integrating the number of cells per section to the entire kidney volume. For this purpose, kidney volume was approximated by ellipse volume, according to the equation: $volume = 4/3\pi abc$, where a, b, and c are the axes. The proportion of EPCs that engrafted kidneys and was detectable 2 and 3 weeks after their transplantation (Figure 6B) was limited to 1% to 2% of the number of injected cells. The scarcity of injected EPCs in the kidneys raised the question whether and how these minute numbers of progenitors could be responsible for the observed marked attenuation of AAN. To address this problem, we considered the possibility of (1) paracrine signaling by adoptively transferred EPCs and (2) their participation in a recently described novel mechanism of cell-to-cell communication via the tunneling nanotubes (TNT).[11]

First, we examined the possibility that adoptively transferred EPCs can change the cytokine profile via a paracrine mechanism, as advocated by many investigators (reviewed by Gnecchi et al[12]). Multiplex analysis of proinflammatory cyto- and chemokines revealed that adriamycin resulted in the increased levels of IL-1α, IL-1β, G-CSF, and IL-8 (murine KC; Figure 7, A–D). Infusion of EPCs to adriamycin-treated mice significantly reduced plasma levels of IL-1α and -β, and G-CSF, but increased the level of KC, which is endowed with the ability to mobilize stem cells. In addition, plasma levels of VEGF were further increased by adoptive transfer of EPCs (Fig-

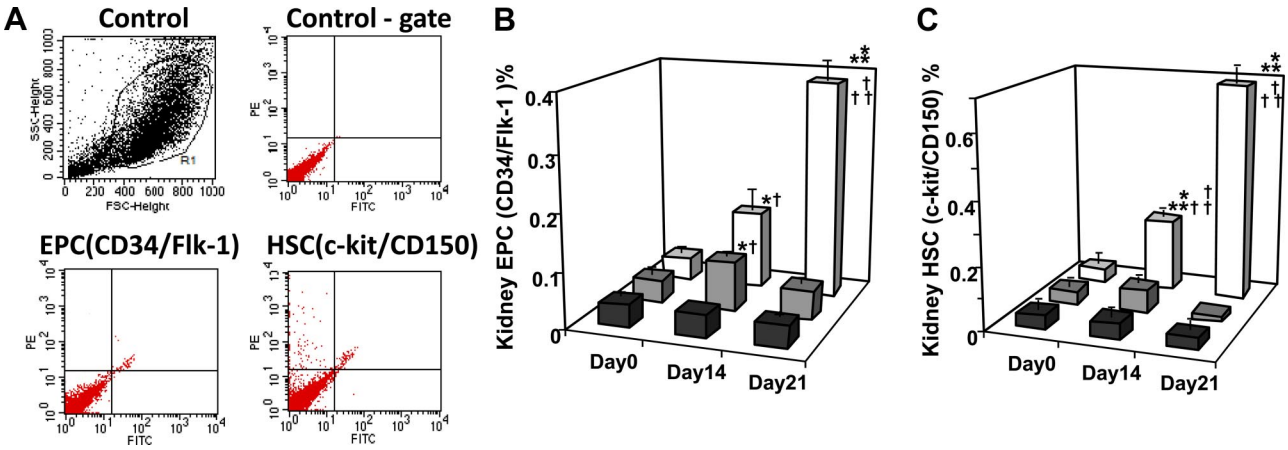

Figure 3. Dynamics of EPCs and HSCs in the kidney during AAN and after adoptive transfer of EPCs. **A:** The forward scatter (FSC)/side scatter (SSC) dot-plot was used to gate kidney cells (**upper left**). Gated cells were displayed in the fluorescence FL1/FL2 (FITC on *x* axis/PE on *y* axis) dot-plot as unstained control (**upper right**). Dot plot of anti–CD34-FITC versus anti–Flk-1–PE fluorescence (**lower left**). Dot plot of anti–c-kit–FITC versus anti–CD150-PE fluorescence (**lower right**). **B:** Proportion of EPCs after administration of adriamycin. **C:** Proportion of HSCs after administration of adriamycin. $^{*}P < 0.05$ versus control and $^{**}P < 0.05$ versus adriamycin, respectively; $^{\dagger}P < 0.05$ versus Day 0 and $^{\dagger\dagger}P < 0.05$ Day 14, respectively ($n = 35$). Black bars indicate control; gray bars, adriamycin; white bars, adriamycin followed by adoptive transfer of EPCs.

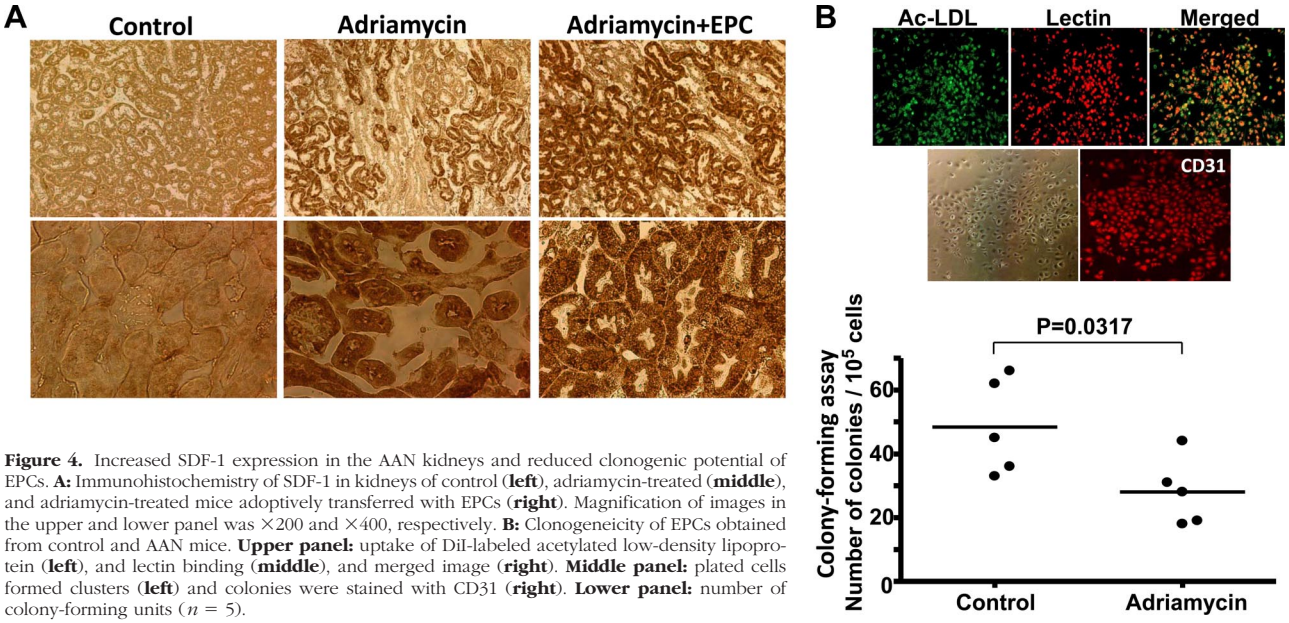

Figure 4. Increased SDF-1 expression in the AAN kidneys and reduced clonogenic potential of EPCs. **A:** Immunohistochemistry of SDF-1 in kidneys of control (**left**), adriamycin-treated (**middle**), and adriamycin-treated mice adoptively transferred with EPCs (**right**). Magnification of images in the upper and lower panel was ×200 and ×400, respectively. **B:** Clonogeneicity of EPCs obtained from control and AAN mice. **Upper panel:** uptake of DiI-labeled acetylated low-density lipoprotein (**left**), and lectin binding (**middle**), and merged image (**right**). **Middle panel:** plated cells formed clusters (**left**) and colonies were stained with CD31 (**right**). **Lower panel:** number of colony-forming units ($n = 5$).

ure 7E). This was accompanied by the restoration of microvascular density in the affected kidneys, as judged by the analysis of CD31 and von Willebrand factor staining of the kidney cryosections (Figure 8A) and reduced frequency of TUNEL-positive cells (Figure 8B). Based on these findings it can be argued that changes in cyto- and chemokine profile could have contributed to the therapeutic effect of adoptively transferred EPCs.

Recently, a novel pathway of cell-to-cell communication comprising the formation of TNT has been described.[11] TNT were shown to facilitate selective transfer of organelles between distant cells. This mechanism accounts for mitochondrial transfer between adult stem cells and somatic cells rescuing their respiration.[13] By all existing accounts, this mechanism, although difficult to demonstrate *in vivo* and therefore studied in cultured cells, should play a significant role in intercellular communication.[14] Based on these studies we endeavored to examine the possibility of existence of TNT mechanism in endothelial cells subjected to adriamycin and presented with EPCs. Subconfluent human umbilical vein endothelial cells (HUVECs) were exposed to 1 μmol/L adriamycin for 1 hour, labeled with CFDA SE, and washed with fresh culture medium. EPCs were labeled with Mitotracker,

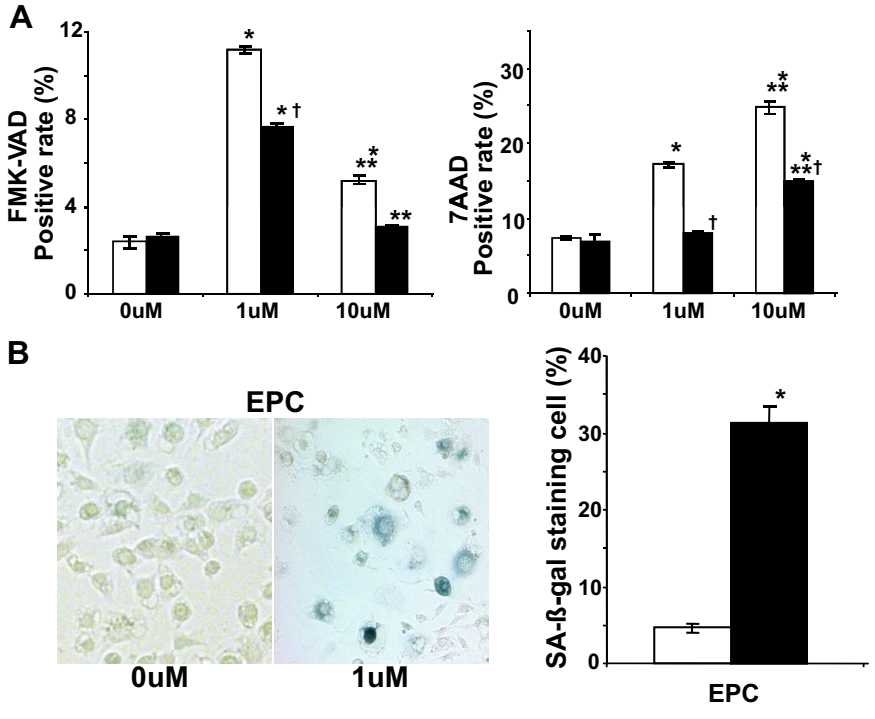

Figure 5. Adriamycin reduces viability and induces senescence of EPCs. **A:** Rate of apoptotic (**left**) and nonapoptotic (**right**) death of EPCs harvested from the bone marrow of BALB/c and C57/BL6 mice. X-bar showed each dosage of adriamycin. Cells were harvested and stained 24 hours after adriamycin injection, then analyzed by FACS. $^{*}P < 0.05$ versus 0 μmol/L, $^{**}P < 0.05$ versus 1 μmol/L. $^{\dagger}P < 0.05$ versus C57/BL6. White bar indicates C57/BL6; black bar, BALB/c mice. **B:** Representative images and quantitative summary of stress-induced premature senescence of EPCs. Cells were subjected to adriamycin for 2 hours and stained for senescence-associated β-galactosidase 5 days later. $^{*}P < 0.05$ vs. 0 μmol/L. White bar: 0 μmol/L, black bar 1 μmol/L.

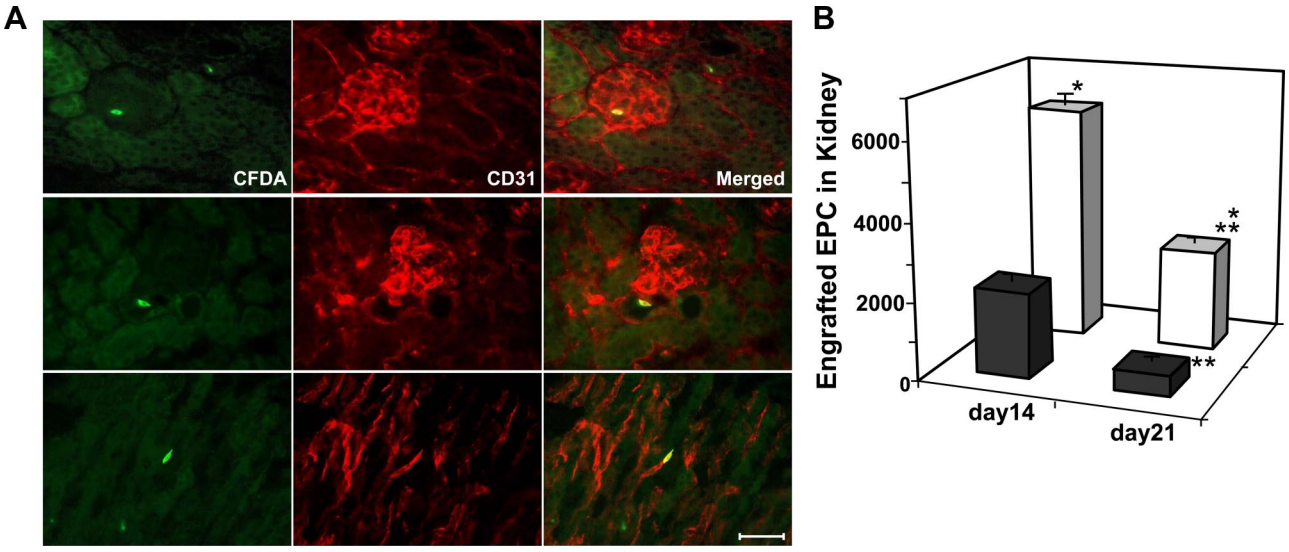

Figure 6. Representative images and quantitative analysis of labeled EPCs engrafting the AAN kidneys. **A:** CFDA-labeled EPCs (**left**); CD31 immunohistochemistry (**middle**); merged images (**right**). **Upper panel:** labeled transferred cells in the glomerulus; **middle panel:** afferent arteriole; **lower panel:** vasa recta. Scale bar = 50 μm. **B:** The approximate number of EPCs engrafting the kidney in AAN was quantified by integrating the number of cells per section (10 μm) to the entire kidney volume. See text for the detailed description. $^{*}P < 0.05$ versus control+EPC and $^{**}P < 0.05$ versus day 14. Black bars indicate control+EPC; white bars, adriamycin+EPC.

washed, and presented to HUVEC cultures at one-tenth of HUVEC density. (In companion experiments, the labeling with fluorophores was reversed: HUVECs were labeled with Mitotracker and EPCs with CFDA SE). As illustrated in Figure 9A, multiple TNT were observed between EPCs and HUVECs, accompanied by the exchange of fluorophores. Notably, despite the scarcity of EPCs, the number of HUVECs labeled with the fluorophore loaded into EPCs much exceeded the number of EPCs present in the co-culture (Figure 9B). This observation was further confirmed by FACS analysis (Figure 9C), which showed that 16.7 ± 0.9% of HUVECs have received the fluorophore from EPCs. Because it has been demonstrated that adriamycin cytotoxicity is in part due to developing mitochondrial dysfunction, we next examined the possibility that EPCs could renew mitochondrial pool in affected HUVECs. When EPCs were labeled with MitoTracker, the proportion of adriamycin-treated HUVECs acquiring this tracer reached 34.3 ± 1.2%, suggesting the transference coefficient from EPCs to HUVECs of about 1:3. This process was by and large unidirectional, because MitoTracker-labeled HUVECs did not significantly enrich EPCs with this tracer (not shown). These data strengthen the hypothesis that a small number of EPCs could repetitively engage a much larger population of adriamycin-stressed HUVECs and potentially rescue them. If similar processes occur *in vivo*, this mechanism could

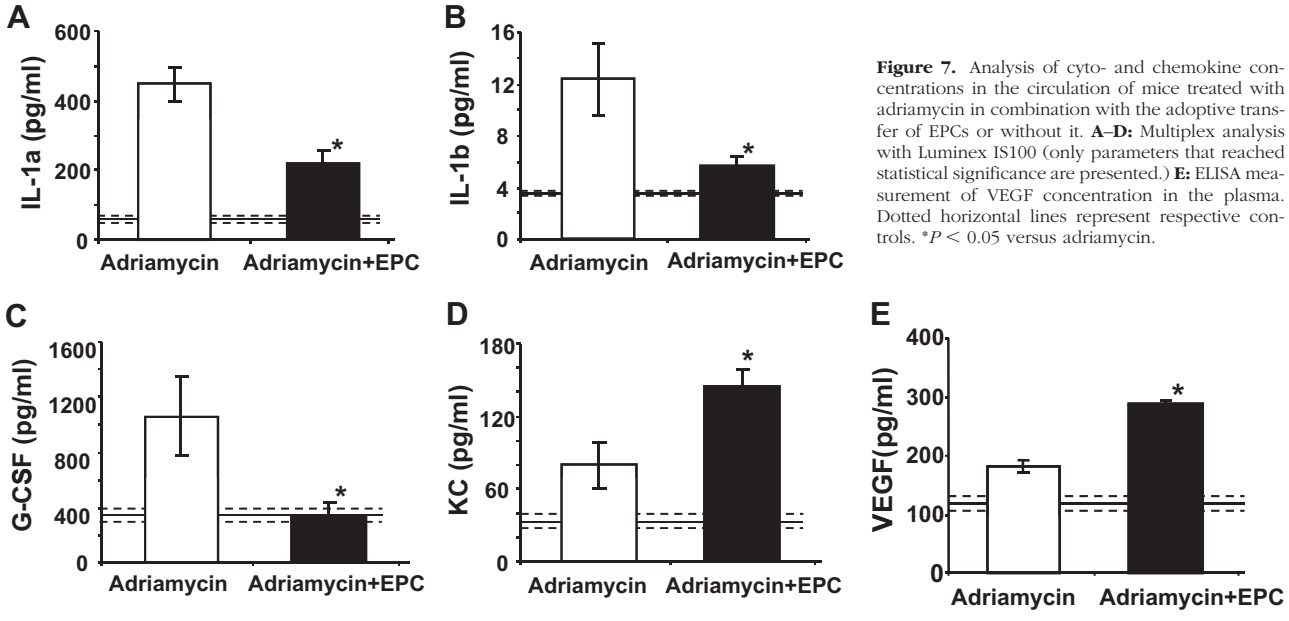

Figure 7. Analysis of cyto- and chemokine concentrations in the circulation of mice treated with adriamycin in combination with the adoptive transfer of EPCs or without it. **A–D:** Multiplex analysis with Luminex IS100 (only parameters that reached statistical significance are presented.) **E:** ELISA measurement of VEGF concentration in the plasma. Dotted horizontal lines represent respective controls. $^{*}P < 0.05$ versus adriamycin.

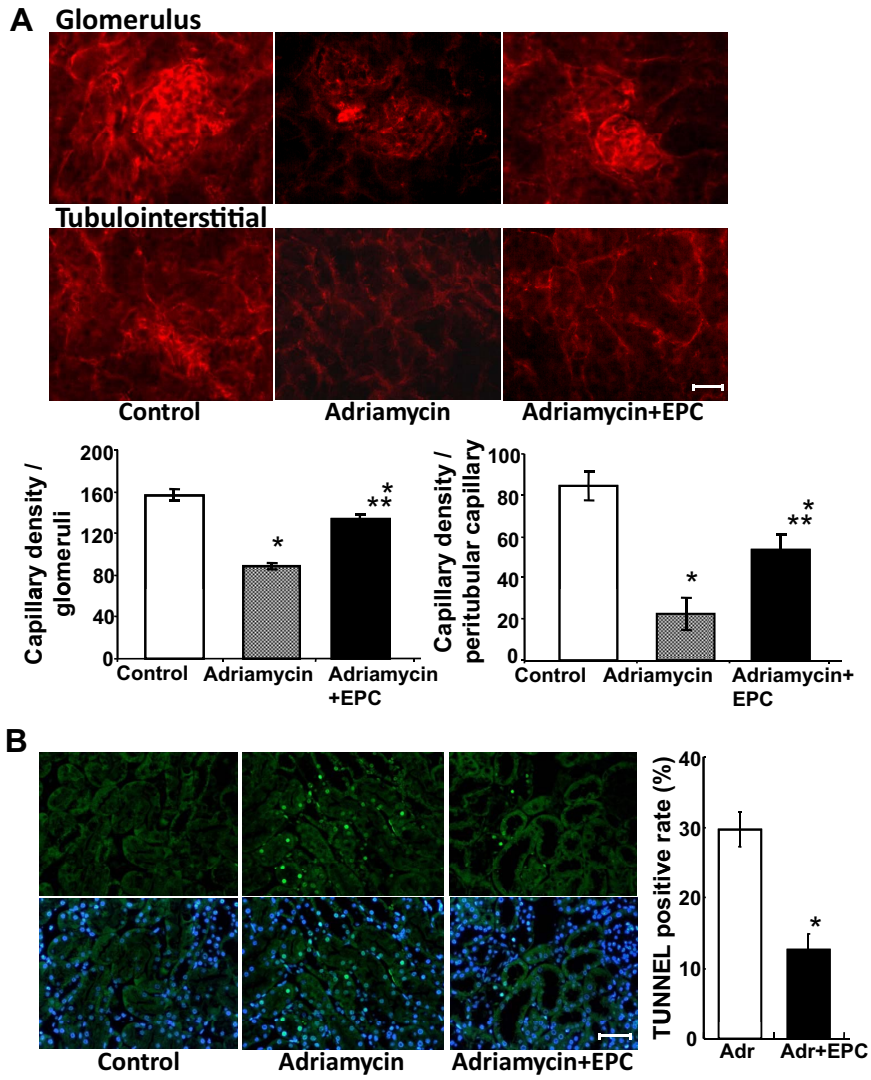

Figure 8. EPC treatment restores microvascular density and reduces the frequency of apoptosis in AAN kidneys. **A:** Representative images of kidney sections stained for CD31. **Upper panel:** glomeruli; **lower panel:** tubulointerstitium. Control, **left**; adriamycin, **middle**; and adriamycin followed by adoptive transfer of EPCs, **right**. Graphs summarize capillary density in each group. Image analysis was performed using National Institutes of Health Image J software. The procedure included threshold image intensity adjustment that enabled identification of microvasculature and quantification of pixels. $^{*}P < 0.05$ versus control and $^{**}P < 0.05$ versus adriamycin. Scale bar = 50 μm. **B:** Representative images of the TUNEL staining of kidney sections. **Upper panel:** TUNEL-positive cells; **lower panel:** merged image of nuclear staining with DAPI. Control, **left**; adriamycin, **middle**; and adriamycin followed by adoptive transfer of EPCs, **right**. TUNEL-positive cells were observed mainly in the outer medulla. Bar diagram summarizes the frequency of TUNEL-positive cells. $^{*}P < 0.05$ versus adriamycin. Scale bar = 50 μm.

explain why a relatively modest number of engrafted EPCs could improve renal function in AAN.

Discussion

The data presented herein provide a conceptual link between the adriamycin-induced stem/progenitor cell apoptotic death and development of their functional incompetence that hampers the engraftment of the kidney and the progressive nature of adriamycin-associated nephropathy. Adoptive transfer of EPCs after adriamycin injection significantly modifies the course of AAN: proteinuria and plasma creatinine concentration are decreased and survival of animals improves. This functional improvement is accompanied by the definitive signs of morphological recovery and reduced levels of pro-inflammatory cytokines. Infused EPCs engrafting adriamycin kidneys are detectable along the microvasculature and, to a lesser degree, in the interstitium of the affected kidneys and their adoptive transfer results in the numerical increase in the population of HSCs and EPCs in the kidneys. Collectively, these lines of investigation provide strong circumstantial evidence favoring the hypothesis that stem cell, and endothelial progenitor cell specifically, injury by adriamycin is in part responsible for the regenerative failure and progressive nature of kidney disease.

Deleterious effects of adriamycin on glomerular endothelial cells have been linked to the development of proteinuria.[15] Vascular dysfunction manifesting in blunted responses to acetylcholine was also demonstrated in *in vitro* studies of isolated thoracic aorta obtained from adriamycin-injected rats,[16] arguing in favor of the developing endothelial dysfunction. Previous studies of adriamycin nephropathy showed that bone marrow–derived cells engrafted the kidneys, and transdifferentiated into endothelial cells and myofibroblasts, which co-expressed endothelial markers suggestive of endothelial-mesenchymal transformation.[17] Yet other investigations, albeit in ischemic kidneys, failed to detect any significant contribution of bone marrow–derived cells to kidney repair.[18,19]

Stressor-induced mobilization of stem cells is common. The surge in stem cells is usually, but not always, associated with regenerative potential. EPCs have been

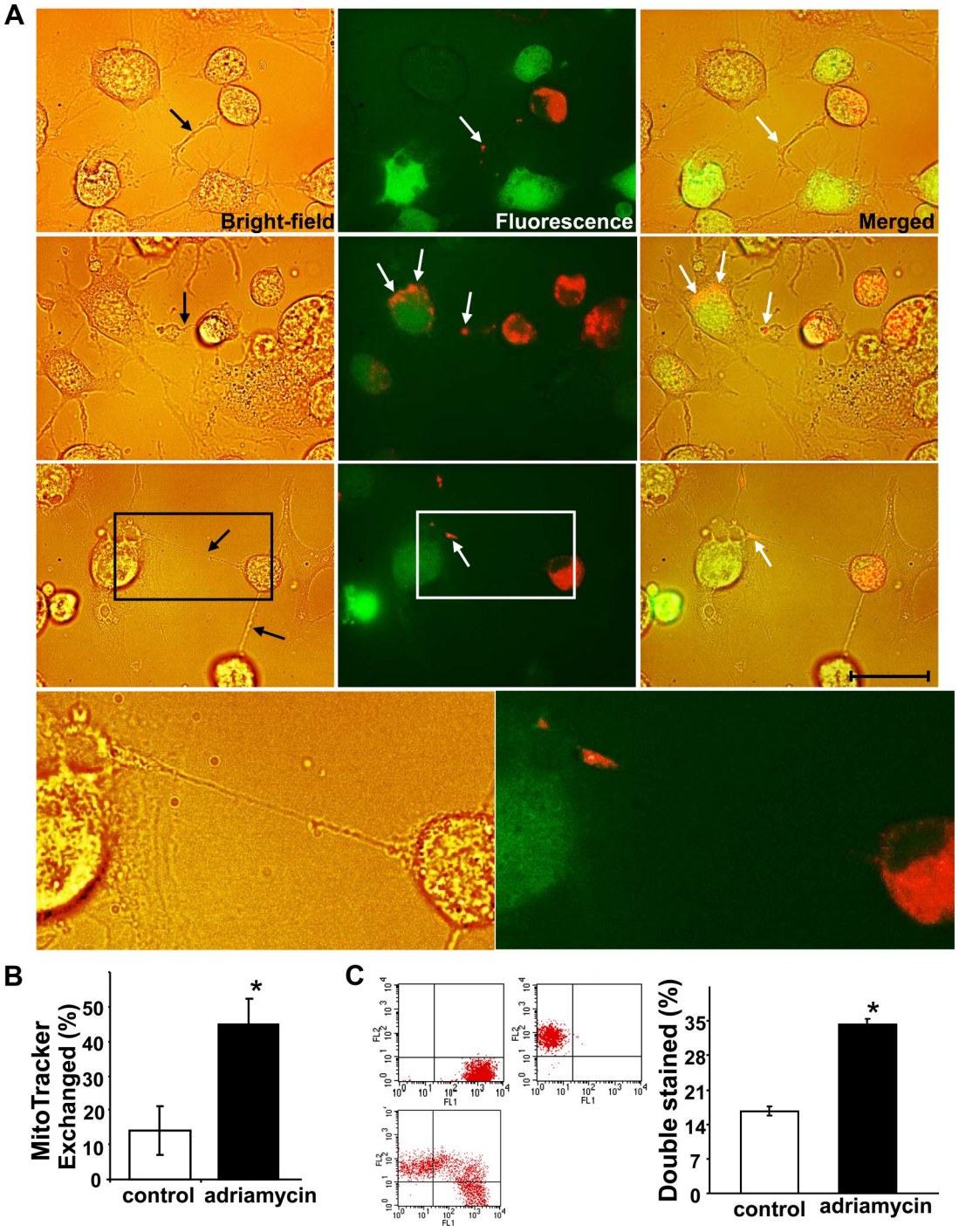

Figure 9. Formation of TNT between intact EPCs and adriamycin-treated HUVECs resulting in mitochondrial exchange. **A:** A gallery of representative bright-field (**left**) and merged fluorescence images (**middle**) and merged fluorescence and bright-field images (**right**) demonstrating TNT after 24 hours in coculture of CDFA-labeled HUVECs (green fluorescence) and Mitotracker-labeled EPCs (red fluorescence). **Black** and **white arrows** show TNT and mitochondrial particles, respectively. Bar = 50 μm. The **bottom panel** shows magnified images of the boxed region above. **B:** Exchange rate of Mitotracker (red fluorescence) quantified with fluorescence microscopy. **C:** Exchanged rate of Mitotracker analyzed by FACS analysis. Dot plot illustrating separate HUVEC staining with CFDA (**upper left**), EPC staining with Mitotracker (**upper right**), and after 24 hours in coculture (**lower**; FL1/FL2: green fluorescence, *x* axis/red fluorescence, *y* axis). **Right panel:** bar diagram summarizing results of FACS analysis of double-stained (denoting that exchange occurred) HUVECs under control conditions and after adriamycin treatment. $^*P < 0.05$ versus control.

shown to participate in regenerative processes. Transplantation of EPCs augments neovascularization of ischemic/infarcted myocardium, ischemic limbs, or brain.[20,21] EPCs may play a critical role in the maintenance of integrity of vascular endothelium and in its repair after injury or inflammation.[22] EPCs are subjected to various stressors, similar to all somatic cells, which could impair their competence.[23] Hyperglycemia has been reported to reduce survival and impair function of circulating EPCs.[24] There is emerging evidence that senescence may serve as an

important mechanism mediating EPC dysfunction. Decreased numbers and increased proportion of senescent EPCs has been reported in patients with preeclampsia or hypertension.[24] Angiotensin II can induce EPC senescence through the induction of oxidative stress and influence telomerase activity.[25] Oxidized low-density lipoprotein induces EPC senescence and dysfunction.[26] In addition, EPC dysfunction has been documented in type I and II diabetes, coronary artery disease, atherosclerosis, vasculitis with kidney involvement, and end-stage renal disease.[27–31]

In this particular situation, AAN, the surge in renal EPCs is either short-lived or decapitated. One of the main reasons for that is reduced viability of endogenous EPCs, their premature senescence and functional incompetence, as judged by the higher frequency of apoptosis, staining for senescence-associated β-galactosidase and reduced clonogenic potential. The fact that exogenous intact EPCs improve structural and functional consequences of adriamycin administration not only further supports the role of these cells in kidney regeneration, but also argues in favor of EPC competence as the necessary prerequisite in accomplishing regenerative functions. Because of the highly heterogeneous population of HSCs and the ability of the monocytic cells to differentiate toward endothelial lineage, it is much more challenging to derive meaningful conclusions from the observed surge in HSCs after EPC transplantation.

Although these studies did not intend to directly address the mechanistic aspect(s) of EPC-mediated regeneration in adriamycin nephropathy, several assumptions can be offered based on the sites of engraftment, results of cyto- and chemokine analyses, VEGF levels and vascular density in the kidneys, and *in vitro* findings of tunneling nanotubes between EPCs and HUVECs. Morphological analysis showed structural improvement of adriamycin nephropathy when EPCs were adoptively transferred. This was also associated with the elevation of plasma VEGF levels and improvement in microvascular density. Adoptive transfer of EPCs was also associated with the reduction in plasma levels of IL-1α and -β, potent pro-inflammatory cytokines, and concomitant reduction of the frequency of apoptosis. Elevation in plasma KC levels after adoptive transfer of EPCs may be of interest as it has not only pro-inflammatory effects but is also capable of mobilizing stem cells and exerting paracrine mitogenic effect, thus potentially explaining the surge in HSCs after EPC infusion.[32,33]

Adriamycin toxicity has been ascribed in part to the mitochondrial dysfunction because of the production of reactive oxygen species.[34,35] In this vein, a newly described formation of tunneling nanotubes is of special interest. Nanotubes were readily formed between EPCs and cultured mature endothelial cells. Fluorophore labeling of the mitochondrial compartment in each cell type showed exchange of mitochondria, which occurred predominantly in the direction from the intact EPCs to the affected HUVECs. This process resulted in the much larger population of HUVECs subjected to nanotube exchange than the actual number of EPCs, indicating that a single EPC could provide organellar exchange to multiple mature adriamycin-injured cells through repeated rounds of tunneling nanotube exchange. The transference number in this case was approximately one EPC to three HUVECs.

In conclusion, AAN is associated with development of EPC apoptosis and premature senescence leading to poor engraftment of the kidney, whereas adoptive transfer of intact EPCs at the onset of AAN blunts its morphological and functional manifestations through direct engraftment, paracrine signaling and, probably, via a TNT-mediated mitochondrial transfer.

References

1. Burke J, Laucius J, Brodovsky H, Soriano R: Doxorubicin hydrochloride-associated renal failure. Arch Intern Med 1977, 137:385–388
2. Guest I, Uetrecht J: Drugs toxic to the bone marrow that target the stromal cells. Immunopharmacology 2000, 46:103–112
3. Couture L, Nash J, Turgeon J: The ATP-binding cassette transporters and their implication in drug disposition: a special look at the heart. Pharmacol 2006, Rev 58:244–258
4. Turnberg D, Lewis M, Moss J, Xu Y, Botto M, Cook T: Complement activation contributes to both glomerular and tubulointerstitial damage in adriamycin nephropathy in mice. J Immunol 2006, 177:4094–4102
5. Kramer A, Hoven van den M, Rops A, Wijnhoven T, Heuvel van den L, Lensen J, Kuppevelt van T, Goor van H, Vlag van den J, Navis G, Berden J: Induction of glomerular heparanase expression in rats with adriamycin nephropathy is regulated by reactive oxygen species and the renninangiotensin system. J Am Soc Nephrol 2006, 17:2513–2520
6. Li J, Campanale N, Liang R, Deane J, Bertram J, Ricardo S: Inhibition of p38 mitogen-activated protein kinase and transforming growth factor-beta 1/Smad signaling pathways modulates the development of fibrosis in adriamycin-induced nephropathy. Am J Pathol 2006, 169:1527–1540
7. Challen G, Bertoncello I, Deane J, Ricardo S, Little M: Kidney side population reveals multilineage potential and renal functional capacity but also cellular heterogeneity. J Am Soc Nephrol 2006, 17:1896–1912
8. Aicher A, Heeschen C, Mildner-Rihm C, Urbich C, Ihling C, Technau-Ihling K, Zeiher A, Dimmeler S: Essential role of endothelial nitric oxide synthase for mobilization of stem and progenitor cells. Nat Med 2003, 9:1370–1376
9. Hatzopoulos A, Folkman J, Vasile E, Eiselen G, Rosenberg R: Isolation and characterization of endothelial progenitor cells from mouse embryos. Development 1998, 125:1457–1468
10. Chen J, HC Park, E Pelger, H Li, M Plotkin, MS Goligorsky: Mesenchymal stem cells participate in vasculogenesis, angiogenesis and endothelial repair. Kidney Interntl 2008, 74:879–889
11. Rustom A, Saffrich R, Markovic I, Walther P, Gerdes HH: Nanotubular highways for intercellular organelle transport. Sci 2004, 303:1007–1010
12. Gnecchi M, Zhang Z, Ni A, Dzau VJ: Paracrine mechanisms in adult stem cell signaling and therapy. Circ Res 2008, 103:1204–1219
13. Spees J, Olson S, Whitney M, Prockop D: Mitochondrial transfer between cells can rescue aerobic respiration. Proc Natl Acad Sci USA 2006, 103:1283–1288
14. Gurke S, Barroso J, Gerdes HH: The art of cellular communication: tunneling nanotubes bridge the divide. Histochem Cell Biol 2008, 129: 539–550
15. Jeansson M, Bjorck K, Tenstad O, Haraldson B: Adriamycin alters glomerular endothelium to induce proteinuria. J Am Soc Nephrol 2009, 20:114–122
16. Ulu N, Buikema H, van Gilst W, Navis G: Vascular dysfunction in adriamycin nephrosis: different effects of adriamycin exposure and nephrosis. Nephrol Dial Transplant 2008, 23:1854–1860
17. Li J, Deane J, Campanale N, Bertram J, Ricardo S: The contribution of bone marrow-derived cells to the development of renal interstitial fibrosis. Stem Cells 2007, 25:697–706
18. Duffield J, Park K, Hsiao L, Kelley V, Scadden D, Ichimura T, Bonventre J: Restoration of tubular epithelial cells during repair of the postischemic kidney occurs independently of bone marrow-derived stem cells. J Clin Invest 2005, 115:1743–1755

19. Lin F, Moran A, Igarashi P: Intrarenal cells, not bone marrow-derived cells, are the major source for regeneration in postischemic kidney. J Clin Invest 2005, 115:1756–1764
20. Asahara T, Murohara T, Sullivan A, Silver M, van der Zee R, Li T, Witzenbichler B, Schatteman G, Isner JM: Isolation of putative progenitor endothelial cells for angiogenesis. Science 1997, 275:964–967
21. Zhang ZG, Zhang L, Jiang Q, Chopp M: Bone marrow-derived endothelial progenitor cells participate in cerebral neovascularization after focal cerebral ischemia in the adult mouse. Circ Res 2002, 90:284–288
22. Minamino T, Miyauchi H, Yoshida T, Ishida Y, Yoshida H, Komuro I: Endothelial cell senescence in human atherosclerosis: role of telomere in endothelial dysfunction. Circulation 2002, 105:1541–1544
23. Rauscher FM, Goldschmidt-Clermont PJ, Davis BH, Wang T, Gregg D, Ramaswami P, Pippen AM, Annex BH, Dong C, Taylor DA: Aging, progenitor cell exhaustion, and atherosclerosis. Circulation 2003, 108:457–463
24. Krankel N, Adams V, Linke A, Gielen S, Erbs S, Lenk K, Schuler G, Hambrecht R: Hyperglycemia reduces survival and impairs function of circulating blood-derived progenitor cells. Arterioscler Thromb Vasc Biol 2005, 25:698–703
25. Sugawara J, Mitsui-Saito M, Hayashi C, Hoshiai T, Senoo M, Chisaka H, Yaegashi N, Okamura K: Decrease and senescence of endothelial progenitor cells in patients with preeclampsia. J Clin Endocrinol Metab 2005, 90:5329–5332
26. Imanishi T, Moriwaki C, Hano T, Nishio I: Endothelial progenitor cell senescence is accelerated in both experimental hypertensive rats and patients with essential hypertension. J Hypertens 2005, 23:1831–1837
27. Vasa M, Fichtlscherer S, Aicher A, Adler K, Urbich C, Martin H, Zeiher AM, Dimmeler S: Number and migratory activity of circulating endothelial progenitor cells inversely correlate with risk factors for coronary artery disease. Circ Res 2001, 89:E1–E7
28. Werner N, Kosiol S, Schiegl T, Ahlers P, Walenta K, Link A, Bohm M, Nickenig G: Circulating endothelial progenitor cells and cardiovascular outcomes. N Engl J Med 2005, 353:999–1007
29. Holmen C, Elsheikh E, Stenvinkel P, Qureshi AR, Pettersson E, Jalkanen S, Sumitran-Holgersson S: Circulating inflammatory endothelial cells contribute to endothelial progenitor cell dysfunction in patients with vasculitis and kidney involvement. J Am Soc Nephrol 2005, 16:3110–3120
30. Chan CT, Li SH, Verma S: Nocturnal hemodialysis is associated with restoration of impaired endothelial progenitor cell biology in end-stage renal disease. Am J Physiol Renal Physiol 2005, 289:F679–F684
31. Choi JH, Kim KL, Huh W, Kim B, Byun J, Suh W, Sung J, Jeon ES, Oh HY, Kim DK: Decreased number and impaired angiogenic function of endothelial progenitor cells in patients with chronic renal failure. Arterioscler Thromb Vasc Biol 2004, 24:1246–1252
32. Schomig K, Busch G, Steppich B, Sepp D, Kaufmann J, Stein A, Schomig A, Ott I: Interleukin-8 is associated with circulating CD133+ progenitor cells in acute myocardial infarction. Eur Heart J 2006, 27:1032–1037
33. He T, Peterson T, Katusic Z: Paracrine mitogenic effect of human endothelial progenitor cells: role of interleukin-8. Am J Physiol 2005, 289:H968–H972
34. Wallace KB: Doxorubicin-induced cardiac mitochondriopathy. Pharmacol Toxicol 2003, 93:105–115
35. Lebrecht D, Walker U: Role of mtDNA in antracycline cardiotoxicity. Cardiovasc Toxicol 2007, 7:108–113